Korean J. Chem. Eng., 37(6), 1029-1035 (2020)
DOI: 10.1007/s11814-020-0508-3

pISSN: 0256-1115
eISSN: 1975-7220

Effects of magnesium loading on ammonia capacity and thermal stability of activated carbons

Ji Hye Park*,‡, Haroon Ur Rasheed,‡, Kwang Hee Cho**, Hyung Chul Yoon***, and Kwang Bok Yi****,†**

*Korea Institute of Industrial Technology, 89, Yangdaegiro-gil, Ipjang-myeon, Seobuk-gu, Cheonan-si Chungcheongnam-do 31056, South Korea
**Graduate School of Energy Science and Technology, Chungnam National University, 99 Daehak-ro, Yuseong-gu, Daejeon 34134, South Korea
***Korea Institute of Energy Research, 140, Yuseong-daero, 1312 beon-gil, Yuseong-gu, Daejeon 34101, South Korea
****Department of Chemical Engineering Education, Chungnam National University, 99 Daehak-ro, Yuseong-gu, Daejeon 34134, South Korea
(*Received 19 October 2019 • accepted 6 February 2020*)

Abstract−Mg-loaded activated carbons were prepared by adding various amounts of Mg (1 to 20 wt%) via ultrasonic-assisted impregnation to investigate the effects on the adsorption and desorption characteristics of ammonia. Mg-loaded activated carbons were characterized by TGA, BET, SEM, EDS mapping, and NH_3-TPD analysis. Mg was homogeneously dispersed on the activated carbon and NH_3-TPD analysis confirmed improved desorption and thermal stability for the 10 wt% Mg sample, named AC-Mg(10). AC-Mg(10) retained the highest desorption for five cycles and showed average desorption amount of 0.788 mmol NH_3/g. During the breakthrough analysis, the AC-Mg(10) showed an initial ammonia adsorption capacity of 0.81 mmol NH_3/g and average adsorption capacity of 0.69 mmol NH_3/g over 30 adsorption and desorption cycles.

Keywords: Activated Carbon, Magnesium, Ammonia, Adsorption, Breakthrough Test

INTRODUCTION

Ammonia (NH_3) is as an essential component of fertilizer production and is needed to support the world's growing population [1]. The industrial-scale synthesis of ammonia from its constituent elements is arguably the most important scientific discovery of the 20th century [1,2]. In 2014, the U.S. Geographic Survey reported that the total worldwide production of ammonia exceeded 1.4 million tons and its demand continues to grow [3]. Ammonia is currently produced through the Haber-Bosch process, where highly pure N_2 and H_2 react at very high temperatures and pressures (300-500 °C and 200-300 atm) over Fe or Ru-based catalysts. However, this process is energy intensive and produces significant carbon emissions. Thus, more environmentally friendly processes are currently being developed [4]. Among the many candidate processes, the chemical or electrochemical synthesis of ammonia is an eco-friendly method for ammonia production. This process has been recently studied by reacting water and atmospheric nitrogen under ambient pressure and relatively low temperatures (<100 °C) [5-8]. However, electrochemical ammonia synthesis produces a relatively low concentration of ammonia compared to the Haber-Bosch process due to its mild reaction conditions. Increasing the conversion rate during the electrochemical synthesis of ammonia is a promising alternative. However, it may also be possible to use an ammonia adsorbent to increase its concentration by repeating ammonia adsorption and desorption. Ammonia gas is toxic and odor-causing, and is commonly removed using various types of adsorbents [9-16]. Most adsorbents for ammonia gas are composed of mesoporous materials such as MOFs [15,17,18], zeolites [18], and activated carbon (AC) [9,10,12,13,19]. AC is widely used for gas purification and can adsorb a number of gases while being abundant and cost-effective [9,10,12,13,19]. AC exhibits large specific surface area as well as porosity and can physically adsorb gas. In addition, chemical adsorption can be achieved mainly by introducing functional groups to the surface to increase adsorption performance.

Guo et al. [12] introduced functional groups to a palm shell-based AC by treatment with H_2SO_4 and correlated the amount of surface oxygen on the AC and ammonia adsorption. Huang et al. [13] compared the ammonia adsorption capacities of coconut shell-based ACs treated with nitric, sulfuric, hydrochloric, phosphoric, and acetic acids. AC treated with nitric acid showed the largest ammonia adsorption capacity, and a linear relationship between ammonia adsorption capacity and acidic functional group content of the adsorbent surface was established. However, functional group introduction via acid treatment of the AC surface greatly increases the adsorption performance for ammonia. Nevertheless, the functional groups are weakened by heat during desorption induced by raising the temperature. Therefore, impregnation with inorganic compounds, such as metals, rather than acid treatment on the surface of AC has been performed [9]. Bandosz and Petit [9] used AC of different origins (coal, wood, and coconut-shell based carbon)

†To whom correspondence should be addressed.
E-mail: cosy32@cnu.ac.kr
‡Both authors contributed equally to this work.

and prepared samples containing various inorganic compounds using impregnation by metal chlorides. These samples were compared under dry and moist conditions, showing that ammonia adsorption capacity depends on the carbon origin, impregnation, and experimental conditions. In addition, a proper combination of surface pH, strength, as well as the type and amount of functional groups present on the adsorbent surface, significantly influence ammonia absorption capacity [9]. Among the inorganic compounds used for impregnation, magnesium (Mg) exhibited a high specific surface area and thermal stability as a catalyst or a support for CO oxidation [20], water gas shift reaction [21,22], and combustion [23,24] requiring a high temperatures. Nevertheless, few studies have been reported regarding the addition of inorganic compounds to AC and their stability and relationship with ammonia gas or between metals or metals oxide and ammonia.

In this study, the enrichment of ammonia produced via electrochemical ammonia synthesis was achieved by repeated adsorption and desorption using the prepared adsorbent. Mg-loaded ACs were prepared by impregnating different amounts of Mg on the AC surface. The characteristics of Mg-loaded ACs were investigated by repeated adsorption and desorption of ammonia. Moreover, the optimum Mg-loaded AC was determined and its thermal stability and long-term operation were tested by repeated adsorption and desorption cycles.

EXPERIMENTAL

1. Sample Preparation

Coconut shell-based AC (GTsx, Shirasagi), known as commercial basic gas adsorbent, was used and washed several times with distilled water to remove surface impurities and dried at 100 °C overnight. Mg-loaded ACs were synthesized by the ultrasonic-assisted impregnation method with different Mg amounts, 1, 3, 7, 10, 15, and 20 wt%. For metal loading on the AC, 0.05 M of aqueous magnesium nitrate hexahydrate was prepared. The resulting slurry was placed in a sonication bath (SD-300H, SEONG DONG) at 80 °C with stirring and maintained until the solvent was completely evaporated. After cooling to room temperature, the product was dried at 100 °C in an oven and calcined in an N_2 environment at 300 °C for 2 h. The prepared adsorbents were designated according to the Mg content as AC, AC-Mg(1), AC-Mg(3), AC-Mg(7), AC-Mg(10), AC-Mg(15), and AC-Mg(20), where AC indicates raw AC and AC-Mg(1) indicates the activated carbon adsorbent and Mg wt%.

2. Breakthrough Test

The ammonia adsorption capacity of the metal-loaded ACs was measured using a fixed bed reactor at room temperature. Before the breakthrough test, the adsorbents were crushed and sieved to a size of 150-300 μm. Subsequently, 0.25 g of the sieved adsorbent was loaded and packed into a 1/4 inch quartz reactor. Before ammonia adsorption, the sample was pretreated at 200 °C for 1 h to remove moisture and the reactor was subsequently cooled to room temperature. A stream of 500 ppm ammonia gas balanced by N_2 was introduced to the reactor at 100 cc/min and passed through the adsorbent bed. The effluent gas was analyzed using an ammonia analyzer (SKT-9300, Korno). Each breakthrough test was stopped when the ammonia concentration at the outlet reached 400 ppm. The desorption process was performed after each breakthrough test for subsequent adsorption by purging the reactor with N_2 at 100 cc/min and increasing the temperature to 200 °C and maintaining the temperature for 1 h.

3. Characterization

The BET surface area and BJH pore size distribution of the prepared adsorbents were measured using an ASAP 2010 analyzer (Micromeritics) with N_2 physisorption isotherms at −196 °C. Before N_2 adsorption, the samples were thermally dried at 200 °C for 4 h under vacuum to remove retained gases and adsorbed water.

The Mg content of the prepared samples was measured by TGA (Thermogravimetric analyzer, TGA-N1000, Sinco). The samples were heated at 10 °C/min to 900 °C in air atmosphere and the flow rate was constant at 100 cc/min.

The surface physical morphology of the samples was examined using a field emission scanning electron microscope (FE-SEM; model Hitachi S-4800). The elemental composition of the sample was determined via SEM/EDX analysis. Energy dispersive analysis by X-ray (EDX) was performed using an X-max 50 instrument. X-ray mapping of C, O, and Mg was performed using an energy dispersive X-ray spectroscope connected to the SEM.

NH_3-TPD (temperature-programmed desorption, BELCAT-M, Bel Japan) was used to measure the extent of desorption from the samples. The sample cell was heated to 350 °C under a flow of He for 1 h. The sample cell was subsequently cooled to 30 °C, and 10 vol% ammonia gas was flowed through the sample cell for 30 min and then flushed with He to remove remaining free ammonia. Finally, the sample cell was heated at a rate of 10 °C/min to 350 °C, while desorbed ammonia was measured with the TCD. The sample cell was cooled to 30 °C and this process was repeated.

RESULTS AND DISCUSSION

Physical characteristics, including specific surface area, pore-volume, and pore size of prepared samples, are shown in Table 1. The specific surface area of the AC was 987 m^2/g and the specific surface area and pore volume of samples changed upon Mg addition. The specific surface area and pore volume increased when a small amount of Mg was impregnated on the AC surface. However, the specific surface area and pore volume decreased for samples impregnated with ≥7 wt% Mg.

Many studies have reported that adding small amounts of Mg to

Table 1. Characteristics of the samples

	Surface area (m^2/g)	Pore volume (cm^3/g)	Pore diameter (Å)
AC	987	0.53	21
AC-Mg(1)	1073	0.57	21
AC-Mg(3)	1019	0.54	21
AC-Mg(7)	842	0.45	21
AC-Mg(10)	691	0.36	21
AC-Mg(15)	568	0.30	21
AC-Mg(20)	521	0.27	21

a catalyst or adsorbent as a promoter or support can improve stability, inhibit sintering, and increase specific surface area [25-27]. Similarly, when a small amount of Mg was added to the AC surface, it served as a support. In contrast, the specific surface area and pore volume decreased at >7 wt% Mg because the solution pH remained constant during the experiment due to fixed molar concentration of the metal precursor. However, with increasing metal (Mg) content, the solvent amount was increased to maintain fix amount of molar concentration (0.05 M). High amount of solution high sonication requires time and temperature to evaporate the solvent, which makes possible for Mg to accommodate in pores. This phenomenon causes blockage of pores that decreases pore volume and the specific surface area. The BJH pore size distributions of the Mg-loaded ACs are shown in Fig. 1 and the average pore size was constant in all samples. Mg loading onto the AC surface did not affect the pore size. Differences in NH_3 capacity of the adsorbents likely originated from differences in surface area and pore volume, but no apparent trends were recognized.

The TGA test was performed by increasing the temperature to 900 °C under an air atmosphere to confirm the Mg content of the

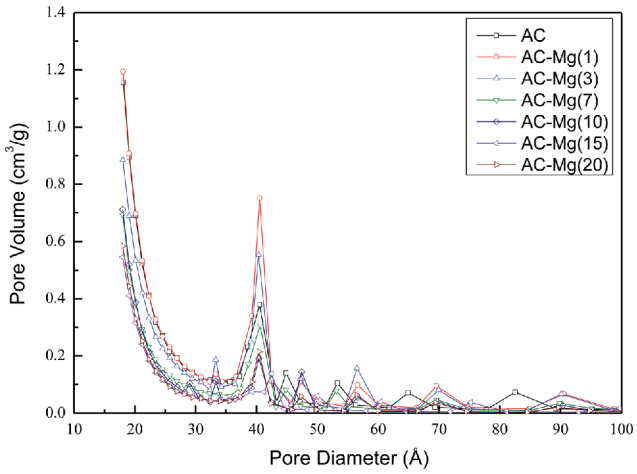

Fig. 1. BJH pore size distributions of raw AC and Mg-loaded ACs.

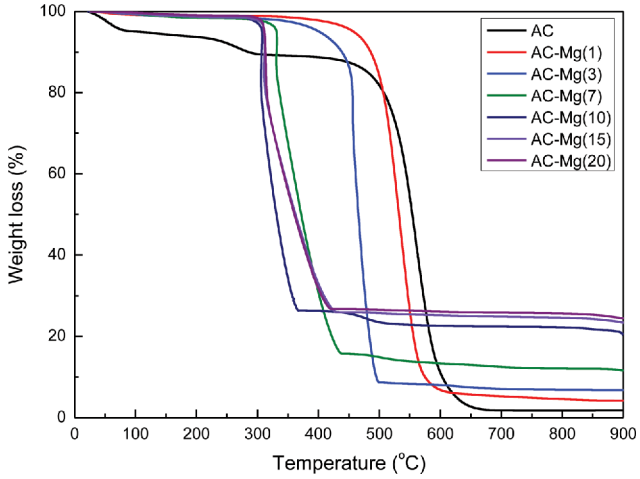

Fig. 2. Thermogravimetric analysis of samples under air condition.

samples synthesized by the ultrasonic-assisted impregnation, as shown in Fig. 2. The AC showed a curve in which water was removed at a temperature of <100 °C. Another weight-loss peak was observed at approximately 230 °C, indicating that the AC surface was successfully acid-treated to produce functional groups, which were removed at this temperature. Silva et al. [28] reported that when the sample of multi-walled carbon nanotubes (MWCNT) was oxidized, the functional groups on the surface of nanotubes, which are hydroxyl (-OH), carbonyl (C=O), and carboxyl (-COOH) groups, were removed at temperatures below 400 °C. This final amount was mostly residues or ash in the form of oxides that combined with oxygen by reaction with air [29]. In contrast, the Mg-loaded AC showed a higher final weight than the unloaded AC, and its final weight increased with increasing metal impregnation. The Mg content was higher than that of the impregnated amount in wt% because Mg reacted with air and remained in the form of magnesium oxide. The similar final weights of AC-Mg(15) and AC-Mg(20) indicate the limit of the Mg content that can be used for impregnation. In addition, the AC loaded with Mg began to show a weight decrease at a lower temperature than AC. Al Amer et al. [30] conducted TGA testing using CNTs and CNT-Fe_2O_3 and confirmed that the CNT-Fe_2O_3 samples reduced the initial and final degradation temperature of the CNTs by approximately 100 °C. It is likely that the lower thermal stability of CNT-Fe_2O_3 compared to that of CNTs is due to the attachment of iron oxide particles to the CNT walls [30]. The results presented herein also showed that the samples of Mg-loaded AC showed a decreased weight at a lower temperature but were stable up to 300 °C because the samples were calcined.

SEM and EDX analyses were performed to examine the surface morphology and impregnation amount more accurately. Fig. 3(a) and (b) shows the SEM images and EDS spectra of the AC and the AC-Mg(10) samples, respectively. The surface of AC-Mg(10) was impregnated with Mg and was more uniform than the AC sample, but no significant difference was observed. The AC, which is a commercial adsorbent, was subjected to surface acid treatment, creating a relatively large oxygen content on the surface. In addition, AC-Mg(10) contained 9.08 wt% of Mg, confirming that Mg well adhered to the sample. Table 2 shows the results of the EDS analyses of AC-Mg(1) and AC-Mg(15). AC-Mg(1) confirmed that Mg was well attached, but for AC-Mg(15), Mg was not fully adhered with a final content of 12.11 wt%. Therefore, the appropriate amount of Mg for the AC used in this study was 10 wt%. In addition, the amount of oxygen increased significantly with Mg impregnation, existing in the form of oxides on the active carbon surface, such as MgO or $Mg(OH)_2$.

Mapping analysis was also performed to ensure that the Mg

Table 2. Element composition through EDS analysis of samples

	C	O	Mg
AC	84.28	15.73	-
AC-Mg(1)	85.78	13.60	0.62
AC-Mg(10)	60.51	30.41	9.08
AC-Mg(15)	51.81	36.08	12.11

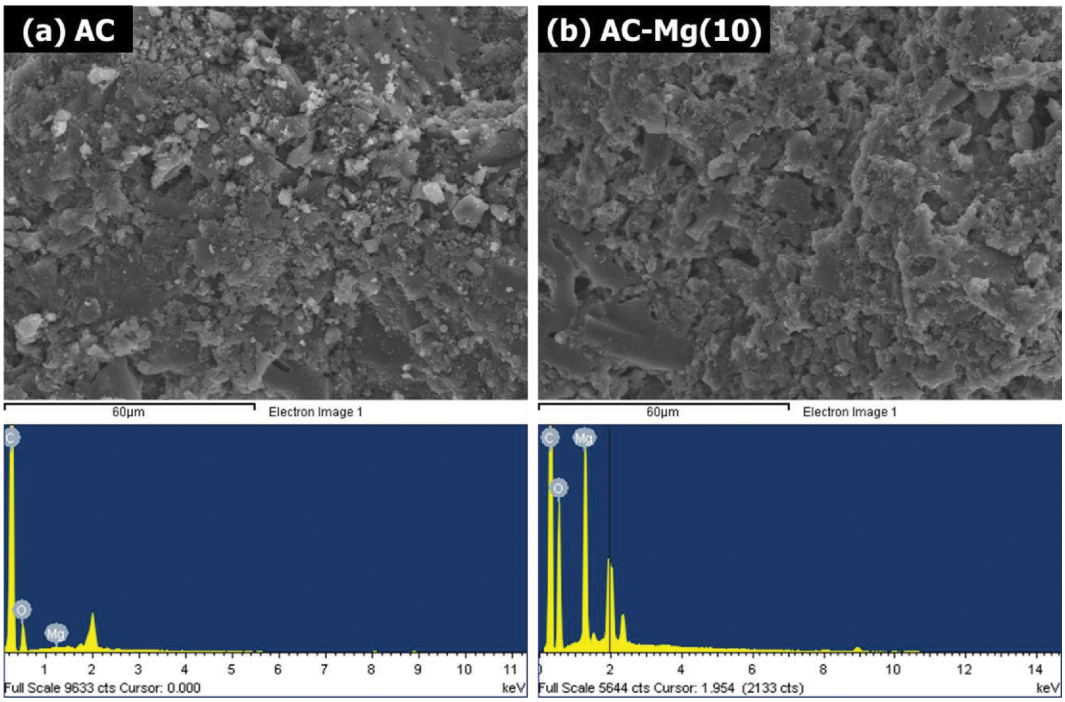

Fig. 3. FE-SEM images and EDS spectra of (a) AC and (b) AC-Mg(10).

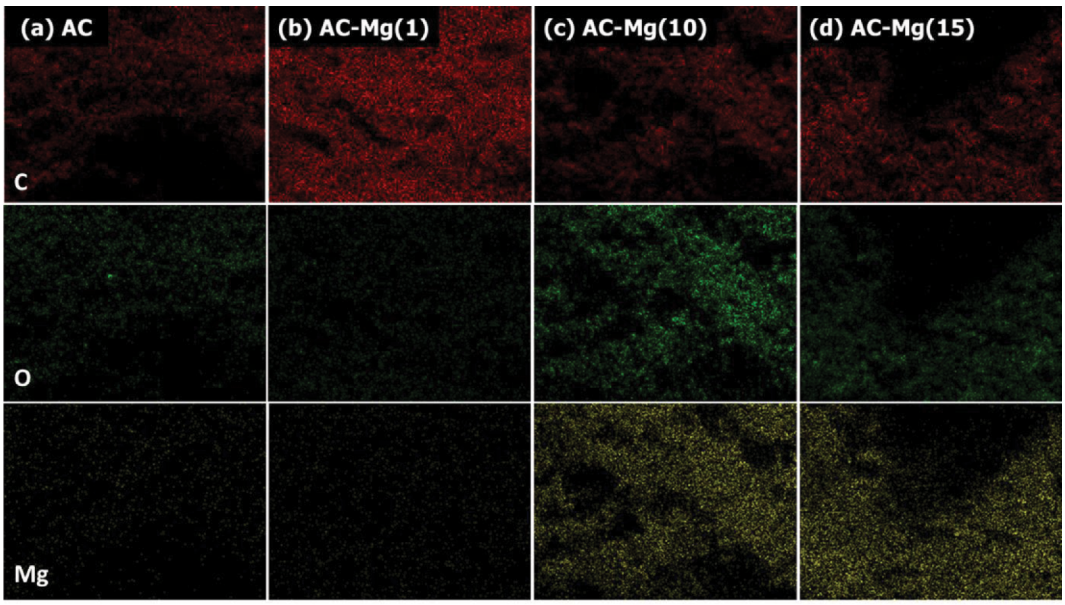

Fig. 4. SEM-mapping of samples.

was uniformly attached to the AC via impregnation (Fig. 4). The EDS mapping showed that the amount of oxygen also increased with increasing Mg content.

NH_3-TPD analysis is generally used to analyze the amount of acid in catalysts [31-33], but, in this study, after ammonia adsorption at room temperature, desorption was determined with increasing temperature, as shown in Fig. 5. Ammonia at a high concentration (10 vol%) was adsorbed to the sample cell for 30 min and subsequently desorbed. The desorbed amount was calculated using the area of 30 to 300 °C. All samples exhibited maximum desorption at approximately 100 °C and the highest desorption amounts were 0.826 and 0.829 mmol NH_3/g for AC-Mg(10) and AC-Mg(15), respectively. The desorption performance of AC was 0.652 mmol NH_3/g higher than that of AC impregnated with ≤7 wt% Mg. The NH_3-TPD results showed increased desorption amount in the following order: AC-Mg(1)<AC-Mg(3)<AC-Mg(7)<AC<AC-Mg(10), AC-Mg(15). Note that, although the peak intensity decreased when the temperature was increased to >300 °C for the AC-Mg series,

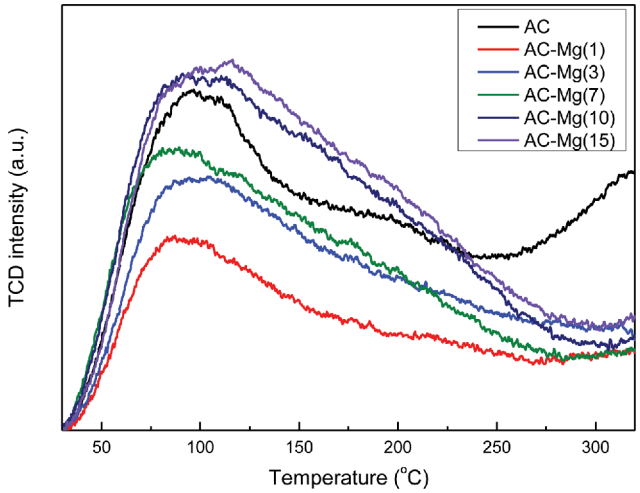

Fig. 5. NH_3-TPD profiles of samples.

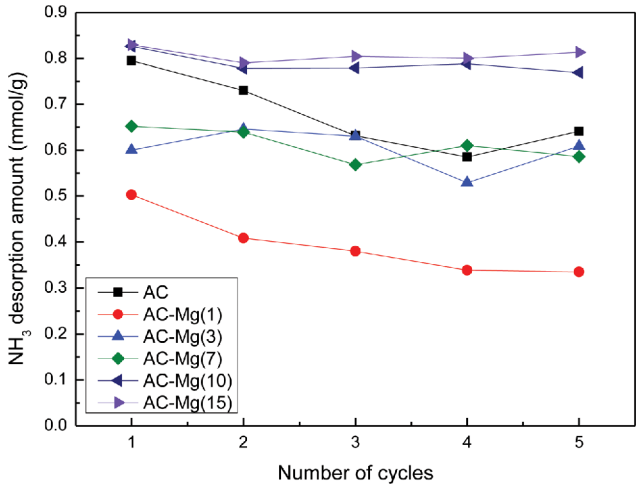

Fig. 6. NH_3-TPD cyclic test of samples.

the peak increased again at >250 °C for AC. The peak at >250 °C for AC corresponded to the point at which the functional groups

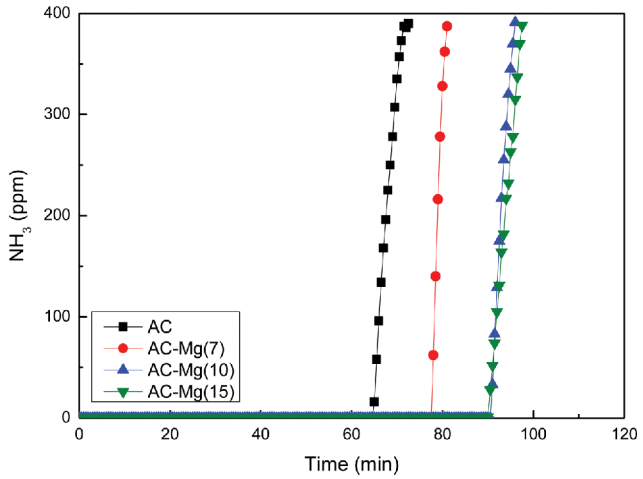

Fig. 7. Breakthrough curves for samples with 500 ppm influent NH_3 under ambient condition.

attached to the AC surface were removed, which is consistent with the TGA results.

Fig. 6 shows the change of desorption amounts obtained by calculating the area and the desorption amounts after repeated NH_3-TPD experiments. AC-Mg(10) and AC-Mg(15) retained high desorption for five cycles of high-temperature desorption at 350 °C and showed average desorption amounts of 0.788 and 0.807 mmol NH_3/g, respectively. AC showed a relatively high desorption amount during the initial desorption test, but the desorption gradually decreased with subsequent cycles. Thus, the functional groups and amorphous carbon on the AC surface were removed during desorption by raising the temperature after the first adsorption, significantly affecting the repeated adsorption and desorption [28]. In contrast, AC-Mg(3) and AC-Mg(7) exhibited smaller amount of desorption than that of AC, but did not show dramatic decreases in desorption amounts during repeated adsorption and desorption cycles. AC-Mg(1) showed the lowest desorption amount.

The breakthrough experiments were performed using the AC, AC-Mg(7), AC-Mg(10), and AC-Mg(15) samples, showing relatively high desorption amounts through the NH_3-TPD analysis, as

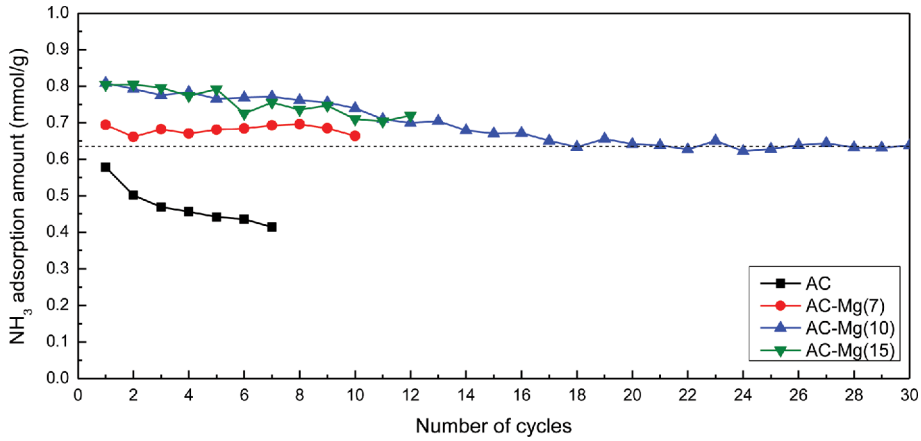

Fig. 8. Breakthrough cyclic test of samples.

shown in Fig. 7. The highest adsorption of ammonia was observed for AC-Mg(10) at 90.5 min (0.81 mmol NH_3/g) and AC-Mg(15) at 90 min (0.80 mmol NH_3/g). The breakthrough time for AC-Mg(7) was 77.5 min (0.69 mmol NH_3/g) and 64.5 min for AC (0.58 mmol NH_3/g). The breakthrough test results of AC-Mg(7), AC-Mg(10), and AC-Mg(15) were similar to those of NH_3-TPD results. In contrast, the adsorption amount of AC was lower than that indicated by the NH_3-TPD results. This difference is due to the removal of amorphous carbon and functional groups on the surface of AC by heating. Thus, AC-Mg(10) was considered to be an optimum sample, considering the amount of Mg added to the AC surface, the adsorption and desorption amounts, and the repetitive cycling tests. Fig. 8 shows the results of the repeated breakthrough experiments with other samples that were used to confirm the thermal stability of the repeated adsorption and desorption of AC-Mg(10). The adsorption amount of AC decreased gradually due to decreasing structural stability of the surface due to the repetitive high-temperature desorption processes. In contrast, the three samples containing Mg showed stable performance despite the repeated adsorption and desorption. AC-Mg(10) showed the highest initial adsorption rate of 0.81 mmol NH_3/g, with a gradually decreasing capacity up to 18 tests, but a constant adsorption capacity from 18 to 30 repetitions without degradation of activity with an average adsorption capacity of 0.69 mmol NH_3/g.

CONCLUSIONS

AC samples were synthesized using an Mg precursor by the ultrasonic-assisted impregnation method and used as adsorbents for ammonia enrichment. The adsorption and desorption characteristics of the Mg-impregnated ACs were compared and analyzed. Addition of a small amount of Mg increased the specific surface area and pore volume of the samples, whereas excess Mg addition reduced the specific surface area and pore volume due to the ultrasonic wave and heat treatments. From the TGA, EDS, and mapping results, the maximum Mg loading that can be impregnated on the AC was determined to be 10 wt%. The desorption amounts were compared and analyzed via NH_3-TPD experiments. AC-Mg(10) and AC-Mg(15) exhibited higher desorption capacity and stability than that of AC. Finally, the AC-Mg(10) was selected as an adsorbent for ammonia concentration as it demonstrated good thermal stability and relatively high ammonia adsorption capacity. After repetitive breakthrough tests for more than 30 cycles, the adsorption performance was well maintained without a significant decrease in activity. The initial adsorption capacity of 0.81 mmol NH_3/g and average adsorption capacity of 0.69 mmol NH_3/g showed that adsorption performance can be improved when Mg is appropriately loaded on the AC surface to retain oxygen in the form of metal oxide. In addition, the thermal stability was improved compared to that of the unloaded acid-treated AC.

ACKNOWLEDGEMENTS

This work was conducted under the framework of the Research and Development Program of the Korea Institute of Energy Research (KIER) (C0-2421). This work was also supported by a research fund of Chungnam National University.

REFERENCES

1. M. A. Shipman and M. D. Symes, *Catal. Today*, **286**, 57 (2017).
2. V. Smil, *Nature*, **400**, 415 (1999).
3. S. Jewell and S. M. Kimball, *US Geological Survey*, **9**, 196 (2015).
4. K. Kim, S. J. Lee, D. Y. Kim, C. Y. Yoo, J. W. Choi, J. N. Kim, Y. Woo, H. C. Yoon and J. I. Han, *ChemSusChem*, **11**, 120 (2018).
5. S. Chen, S. Perathoner, C. Ampelli, C. Mebrahtu, D. Su and G. Centi, *Angew. Chem., Int. Ed.*, **56**, 2699 (2017).
6. E. Y. Jeong, C. Y. Yoo, C. H. Jung, J. H. Park, Y. C. Park, J. N. Kim, S. G. Oh, Y. Woo and H. C. Yoon, *ACS Sustain. Chem. Eng.*, **5**, 9662 (2017).
7. V. Kordali, G. Kyriacou and C. Lambrou, *Chem. Commun.*, **17**, 1673 (2000).
8. J. N. Renner, L. F. Greenlee, K. E. Ayres and A. M. Herring, *Electrochem. Soc. Interface*, **24**, 51 (2015).
9. T. J. Bandosz and C. Petit, *J. Colloid Interface Sci.*, **338**, 329 (2009).
10. M. Ghauri, M. Tahir, T. Abbas, M. S. Khurram and K. Shehzad, *Sci. Int. (Lahore)*, **24**, 411 (2012).
11. M. Gonçalves, L. Sánchez-García, E. d. Oliveira Jardim, J. Silvestre-Albero and F. Rodríguez-Reinoso, *Environ. Sci. Technol.*, **45**, 10605 (2011).
12. J. Guo, W. S. Xu, Y. L. Chen and A. C. Lua, *J. Colloid Interface Sci.*, **281**, 285 (2005).
13. C. C. Huang, H. S. Li and C. H. Chen, *J. Hazard. Mater.*, **159**, 523 (2008).
14. S. D. Kim, E. Magnone, J. H. Park and J. Y. Ryu, *J. Porous Mat.*, **25**, 297 (2018).
15. A. J. Rieth and M. Dincă, *J. Am. Chem. Soc.*, **140**, 3461 (2018).
16. M. Seredych, C. Petit, A. V. Tamashausky and T. J. Bandosz, *Carbon*, **47**, 445 (2009).
17. Y. Chen, F. Zhang, Y. Wang, C. Yang, J. Yang and J. Li, *Micropor. Mesopor. Mater.*, **258**, 170 (2018).
18. Y. Khabzina and D. Farrusseng, *Micropor. Mesopor. Mater.*, **265**, 143 (2018).
19. A. Qajar, M. Peer, M. R. Andalibi, R. Rajagopalan and H. C. Foley, *Micropor. Mesopor. Mater.*, **218**, 15 (2015).
20. L. Molina and B. Hammer, *Phys. Rev. B*, **69**, 155424 (2004).
21. A. M. D. de Farias, A. P. Barandas, R. F. Perez and M. A. Fraga, *J. Power Sources*, **165**, 854 (2007).
22. J. H. Park, J. H. Baek, R. H. Hwang and K. B. Yi, *Clean Technol.*, **23**, 429 (2017).
23. J. I. Baek, J. Ryu, J. B. Lee, T. H. Eom, K. S. Kim, S. R. Yang and C. K. Ryu, *Energy Procedia*, **4**, 349 (2011).
24. M. Zhao, A. I. Minett and A. T. Harris, *Energy Environ. Sci.*, **6**, 25 (2013).
25. V. Choudhary, B. Uphade and A. Mamman, *Catal. Lett.*, **32**, 387 (1995).
26. A. Iriondo, V. Barrio, J. Cambra, P. Arias, M. Güemez, R. Navarro, M. Sánchez-Sánchez and J. Fierro, *Top. Catal.*, **49**, 46 (2008).
27. A. Parmaliana, F. Arena, F. Frusteri, S. Coluccia, L. Marchese, G. Martra and A. Chuvilin, *J. Catal.*, **141**, 34 (1993).
28. W. M. Silva, H. Ribeiro, L. M. Seara, H. D. Calado, A. S. Ferlauto, R. M. Paniago, C. F. Leite and G. G. Silva, *J. Braz. Chem. Soc.*, **23**,

1078 (2012).
29. X. Tian, G. Hong, Y. Liu, B. Jiang and Y. Yang, *RSC Adv.*, **4**, 36316 (2014).
30. A. M. Al Amer, T. Laoui, A. Abbas, N. Al-Aqeeli, F. Patel, M. Khraisheh, M. A. Atieh and N. Hilal, *Mater. Des.*, **89**, 549 (2016).
31. J. H. Baek, J. M. Jeong, J. H. Park, K. B. Yi and Y. W. Rhee, *Trans. Korean Hydrog. New Energy Soc.*, **26**, 423 (2015).
32. J. M. Jeong, J. H. Park, J. H. Baek, R. H. Hwang, S. G. Jeon and K. B. Yi, *Korean J. Chem. Eng.*, **34**, 81 (2017).
33. Z. Wu, R. Jin, Y. Liu and H. Wang, *Catal. Commun.*, **9**, 2217 (2008).